Interpretations of the EOLE Experiment I. Temporal Variation of Eulerian Quantities

PETER J. WEBSTER[1] AND DAVID G. CURTIN

Dept. of Meteorology, University of California, Los Angeles 90024

(Manuscript received 11 March 1974, in revised form 29 April 1974)

ABSTRACT

The recent EOLE constant density balloon experiment, conducted between August 1971 and July 1972 in the upper troposphere of the Southern Hemisphere, produced large quantities of highly accurate Lagrangian data. The question of the inference of Eulerian mean quantities from Lagrangian information is considered, and, in the absence of an exact and general transformation between the two data forms, an approximate method is developed. It is shown that unless sufficient care is taken in this transformation, large errors can occur in the inferred Eulerian estimates by the introduction of a Lagrangian temporal bias into the means. It is suggested that earlier GHOST estimates of the momentum flux by Solot and Angell were abnormally small by a factor of 4 for this reason.

After the elimination of the Lagrangian bias and character, the "Eulerian" data are used to study the temporal variation of various measured and derived quantities which is used to infer the dynamic structure of the hemisphere during the EOLE year. Comparisons are made with estimates derived from conventional data sources and earlier balloon experiments. Large differences are found in regions where the EOLE data are maximum and unbiased longitudinally. It is concluded that many of these differences, for example the Southern Hemisphere double jet stream, may be attributed to the introduction into the conventional data sets of a Eulerian spatial bias due to the longitudinal clustering of the Eulerian sensors.

Finally, the viability of a balloon system to produce meaningful hemispheric data is discussed. It is concluded that while the system seems to represent mid-latitude motion adequately, there is some doubt as to how representative the derived mean tropical atmosphere is for a population of balloons whose maximum density is at higher latitudes.

1. Introduction

The first hemispheric-scale Lagrangian data set resulted from the Southern Hemisphere GHOST experiment where over a period of nearly five years a number of constant level balloons were used to sense the motions of the upper troposphere. The GHOST data set and the implied climatology have been discussed at length by Solot and Angell (1969a,b, 1973) and Angell (1972). These results will be considered later and compared with those obtained from the more extensive EOLE experiment.

With the exception of the GHOST experiments, all other statistics representative of the mean state of the atmosphere have been compiled using data measured relative to a Eulerian observing system. That is, all data were measured relative to a geographically fixed system of observing stations. The major problem with such data is the possibility of contamination by a spatial bias introduced by having more observations in one geographic locale than in another. Such a contamination is often manifested in mean statistics by data aliasing, where spurious power is introduced into the long-wavelength components of the spatial spectra.

The basic data problem of the Southern Hemisphere is illustrated in Table 1a, which shows the number of conventional observing stations (pilot balloon, rawin and radiosonde) reporting in the longitude-latitude grids indicated during the International Geophysical Year (IGY). From each of these stations, Obasi (1963) obtained vertical wind profiles with a frequency maximum of one per day, and at a number of stations temperatures and pressures also. In the upper troposphere, the number of stations regularly reporting 200-mb winds was less than 50 over the entire hemisphere. It is evident that even within the latitudes of maximum observations (equatorward of 35S) there may exist difficulties in the compilation of a meaningful set of statistics because of the longitudinal clustering of the observing stations. This may be seen by the values of the standard deviation of the number of stations, in a 10° latitude belt, normalized by the average number of stations in each 30° longitude box, referred to in Table 1a as C. This quantity is large at all latitudes and indicates the uneveness with longitude of the Eulerian sensors. Statistics compiled using such data are sum-

[1] Present affiliation: Department of Atmospheric Sciences, University of Washington, Seattle 98195.

TABLE 1. Comparison of (a) the number of conventional stations in the Southern Hemisphere reporting during the International Geophysical Year (Obasi, 1963) in the indicated 30° longitude by 10° latitude grid, and (b) the number of velocity determinations from the EOLE data set during November 1971.

a. Distribution of conventional stations: IGY

	Latitude (°S)							
	5	15	25	35	45	55	65	75
Longitude								
15E	3	2	5	1	0	0	0	1
45E	2	6	4	0	1	0	0	0
75E	1	1	0	1	0	0	1	0
105E	2	0	3	1	0	0	2	1
135E	6	6	5	8	1	0	1	0
165E	1	1	1	4	3	0	1	1
165W	1	1	0	0	1	0	0	1
135W	0	1	1	0	0	0	0	0
105W	0	0	0	0	0	0	0	0
75W	4	3	2	3	1	1	0	0
45W	2	0	2	2	0	1	1	1
15W	0	0	0	1	0	0	0	2
Total	22	21	23	21	8	2	7	7
Mean	1.83	1.75	1.92	1.75	0.58	0.17	0.5	0.58
C*	0.98	1.26	1.0	1.34	1.55	2.29	1.35	1.15

b. Number of EOLE velocity determinations in each grid during November 1971

Longitude								
15E	2	17	147	143	171	124	80	1
45E	3	7	164	339	182	221	93	17
75E	2	7	211	414	290	304	138	8
105E	0	1	308	535	355	317	162	20
135E	0	1	81	515	343	277	156	18
165E	0	3	217	540	393	344	185	12
165W	4	39	228	374	351	313	185	14
135W	1	68	214	382	339	280	126	6
105W	4	51	255	241	252	256	101	11
75W	1	26	166	283	223	216	63	2
45W	0	39	125	231	192	222	73	6
15W	3	35	125	203	169	148	49	0
Total	20	294	2241	4200	3260	3022	1409	
Mean	1.67	24.5	186.8	350.0	271.7	251.8	117	
C*	0.93	0.90	0.34	0.38	0.31	0.27	0.40	

* See text for definition.

marized by Newell *et al.* (1972) and van Loon *et al.* (1972).

The EOLE experiment, on the other hand, has resulted in a data set that is comprised of upper tropospheric temperature, pressure and velocity fields which, over a large latitudinal range in the Southern Hemisphere, is not plagued with the same problems as are the Eulerian sets. This may be seen in Table 1b where the number of velocity determinations in each latitude-longitude grid during November 1971 is shown. Poleward of 15S, the values of C represent a much more even distribution in longitude of a larger data population than existed in the Southern Hemisphere during the IGY, the time of maximum conventional observations.

Besides the study of the mean dynamic structure of the upper troposphere Southern Hemisphere, there exists another motivation for undertaking this study. This is the proposed use of constant density balloon systems as atmospheric tracers and instrument bearers in the various forthcoming GARP experiments (e.g., the 1977 First GARP Global Experiment). Consequently, an important part of this study will be the investigation of the transformation of Lagrangian data to an Eulerian form, a problem as important in compilation of a synoptic time-scale data set for use as initial data for a numerical model as for the compilation of a long series of data for the study of the mean structure of the entire hemisphere.

This paper possesses two main areas of focus. The first is the discussion of the treatment of Lagrangian data, and because of the amount of such data that will become available during the next few years, this subject is discussed in some detail in Sections 2 and 3. The remainder of the paper refers to the temporal variation of certain measured and derived fields and their comparison with earlier estimates.

2. The EOLE data set

The EOLE data set resulted from the interrogation of nearly 500 constant density balloons operating on the $\rho = 0.322$ kg m^{-3} isosteric surface, by a satellite in

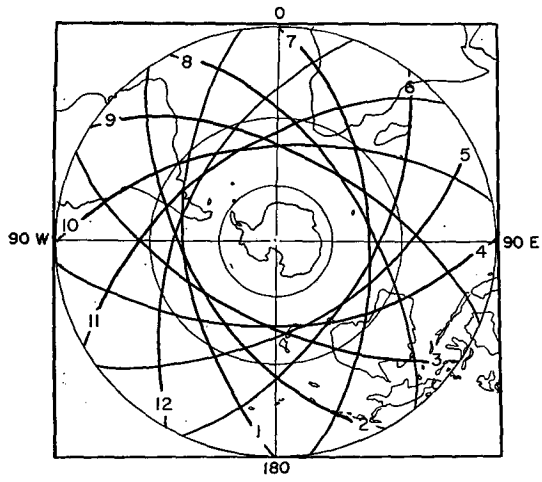

(a)

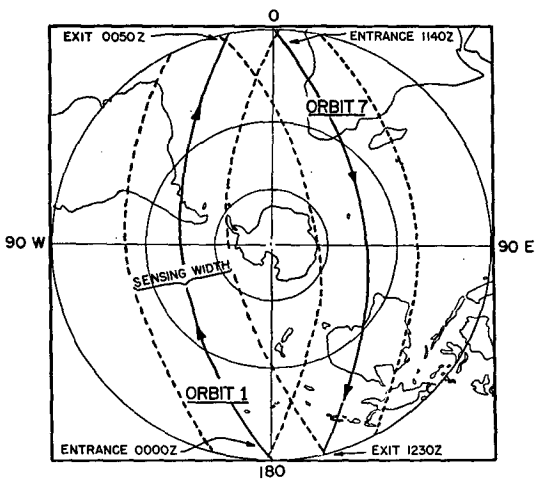

(b)

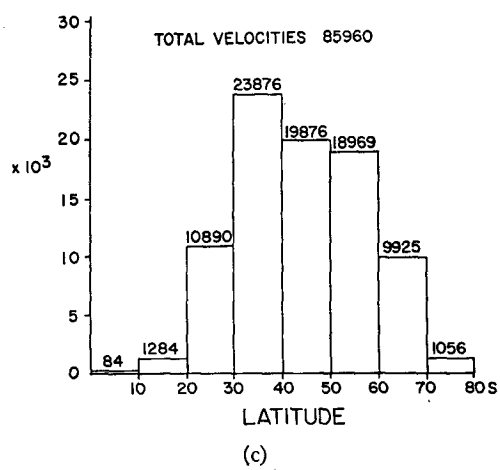

(c)

FIG. 1. Orbital characteristics of the EOLE satellite using (a) all orbits during a 24-hr period and (b) two orbits 12-hr apart. Dashed lines indicate sensing range of satellite. Fig. 1c. Resultant latitudinal distribution of the derived velocities.

a 50° inclined orbit with an orbital time of ~100 min. The isosteric surface closely approximates the 200-mb isobaric surface. Instruments reported the ambient temperature and pressure, and Lagrangian velocities were calculated from balloon displacements between successive satellite orbits. A more complete description of the EOLE experiment is given by Morel and Bandeen (1973).

The character of the data set may be inferred by considering the orbital characteristics of the satellite. In Fig. 1a all orbits during a 24-hr period are superimposed upon a stereographic projection of the Southern Hemisphere. During each orbital pass the satellite crosses the previous orbit in mid-latitudes, although nearly 30° of longitude exists between the entrance points of successive orbits. When the "sensing horizon" of each orbit is considered, as shown in Fig. 1b by the dashed lines about the orbit track, it can be seen that each day the mid-latitude regions are sensed more than the tropics and subtropics and that the polar regions south of 70S are not sensed at all. Fig. 1 suggests the following properties of the EOLE data set:

(i) A balloon in the tropics and subtropics is usually sensed by only one or two consecutive orbits of the satellite to provide only the possibility of an approximately 2-hr (110 min) average Lagrangian velocity. As is evident from Fig. 1b, such a balloon may also be sensed by an orbit nearly 12 hr later sometimes producing two velocities in the 24-hr period but more often only two isolated positions sensed 12 hr apart.

(ii) A balloon in mid-latitudes, on the other hand, may be sensed by up to six consecutive orbits because of the overlapping "sensing horizon" of the satellite allowing a series of consecutive "2-hr" average Lagrangian velocities. However, this will occur only once every 24 hr as the return orbit passes on the other side of the pole.

(iii) A balloon poleward of 70S is never detected, with the result that no data are available south of this latitude which represents the southern limit of the sensing horizon of the satellite.

(iv) The resultant data for a 24-hr period are asynoptic as the balloons are sensed and velocities calculated by the precessing satellite, as may be envisioned from Fig. 1a. However, this asynoptic character is unimportant for the compilation of a set of long-term statistics whose averaging period is very much greater than the precession time of the satellite.

From (i)–(iii) we can see that if the balloon density were constant everywhere over the hemisphere then the velocity determinations would not be. Instead there would be a maximum in mid-latitudes decreasing gradually toward the equator and no observations poleward of 70S. However, the distribution of balloons is not constant in latitude but subject to a broad grouping in mid-latitudes due to a slow meridional

drift imparted to them by the Hadley and Ferrel circulations. The satellite orbit characteristics and the large-scale circulations mentioned explain the distribution of the derived velocities shown in Fig. 1c.

Added to the above effects is the variation of the balloon population during the EOLE year due to the finite life of the balloons. Following the initial launching from three sites in Argentina (33, 39 and 56S), the population of balloons decreased substantially during the following months. From a maximum of nearly 300 balloons aloft in November 1971, the population had decreased to less than 50 in July 1972, as can be seen in Fig. 2a. The distribution of observations as a function of latitude and time is shown in Fig. 2b and shows a poleward shift of the axis of maximum observations through spring and summer with decreasing magnitude.

The accuracy of the derived velocity fields mainly depends upon the accuracy of the location of the balloon by the satellite and results in a velocity error 1–2 m sec^{-1} (Morel and Necco, 1973) which is less than that of conventional Eulerian estimates. The accuracy of temperature and pressure calculations is comparable but equipment failures resulted in far fewer measurements of these quantities than velocities.

A further check was employed to filter out anomalous velocities that may have crept into the data set because of faulty recording or mislabelling of a balloon or satellite orbit. A velocity distribution was compiled for the entire EOLE period and is shown in Fig. 3.

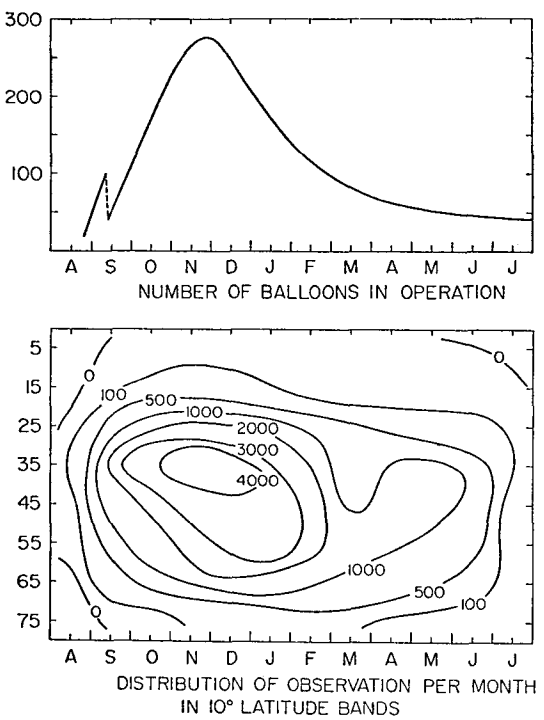

FIG. 2. Monthly variation (a) of the number of operational balloons as a function of time and the total number of observations (b) as a function of latitude and month.

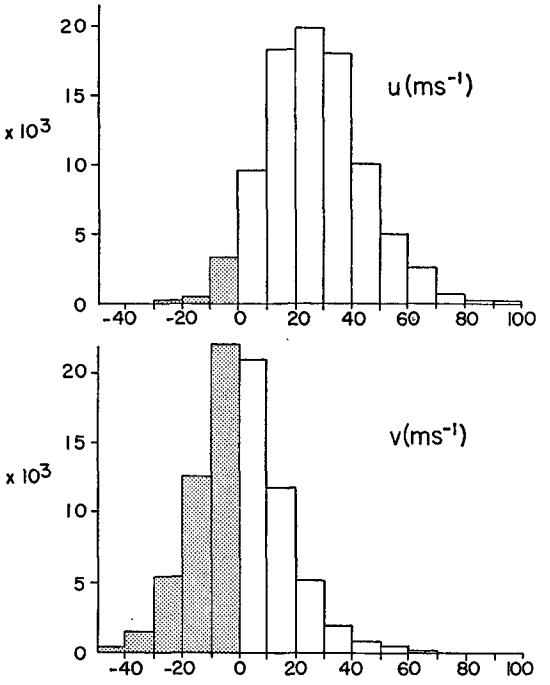

FIG. 3. Distribution of the magnitudes of the meridional and zonal velocity components during the EOLE period.

As the distribution for each component was nearly Gaussian, limits of acceptability were chosen. These were $-30<u<100$ m sec^{-1} and $-60<v<60$ m sec^{-1}. The data passing through this filter were further checked by the consistency of their 2-hr accelerations to eliminate more subtle anomalies.

3. Averaging schemes and data problems

a. Estimation of an Eulerian statistic from Lagrangian measurements

The problem is the determination of Eulerian fields from large quantities of Lagrangian data. (Correctly, the data are "quasi-Lagrangian" because the balloons do not exactly follow fluid parcels but are restricted to remain on surfaces of constant density.) Dyer (1973) has shown that such data transformations are far from trivial and was only able to find exact and analytic transformations for specific atmospheric states, concluding that no general transformation existed. Consequently, in order to use analytic transformations we would require prior information regrading the state of the Eulerian fields and, as this is impossible without first transforming the Lagrangian data, we must resort to less elegant techniques of data treatment.

The problem of inferring the Eulerian from the Lagrangian may be seen from the following simple and exaggerated example. Suppose that the atmosphere is divided into two boxes; a "fast" box (F) with a zonal speed of 50 m sec^{-1} and a "slow" (S) box with a speed of 30 m sec^{-1}. An Eulerian sensor in each box would give

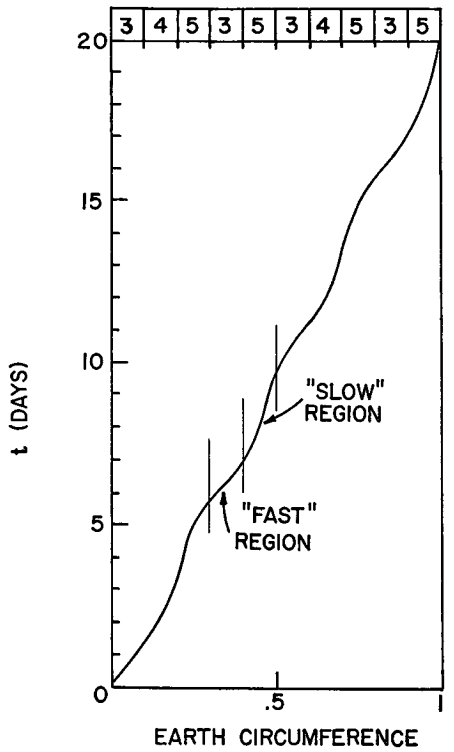

FIG. 4. Longitudinal displacement (x) as a function of time (t) of air parcels for the atmospheric state defined by (1). Numerals indicate the relative number of regular observations in time for each geographically fixed longitudinal box. Space units are normalized to the circumference of the earth.

an average Eulerian zonal wind speed over a particular time period (i.e., a time-space average) of

$$[\bar{u}_E] = (50+30)/2 = 40 \text{ m sec}^{-1},$$

whereas a system of balloons flowing through the system being monitored at regular intervals (as would occur in a real operational Lagrangian system) would find themselves spending less time in F but more time in S simply because they follow the motion of the fluid. Consequently, more observations occur in S than in F. Then if C is the circumference of the earth, the mean Lagrangian wind speed is given by

$$\bar{u}_L = \frac{C}{\text{total time}} = \frac{C}{(\text{time in F}) + (\text{time in S})}$$

$$= 37.5 \text{ m sec}^{-1},$$

which represents a full 5% difference in the zonal wind estimate. Consequently, the equivalence of Eulerian and Lagrangian statistical quantities may not be assumed.

TABLE 2. Various Lagrangian zonal averages of the atmosphere defined by the Lagrangian field [Eq. (1)] using various schemes.

Averaging method	u_L	v_L	uv_L
a. Exact integration			
1. Time averaging [(2) and (3)]	16.4	0	−25.0
2. Time averaging [(2) and (3) with boxes]	17.0	−0.32	−27.6
3. Space averaging [(4) and (5) with and without boxes]	19.5	−1.53	−50.0
b. Numerical integration using 6-hr data with and without boxes			
4. Time averaging (no boxes)	16.4	0	−25.0
5. Time averaging (with boxes)	17.0	−0.03	−29.9
6. Space averaging (no boxes)	17.1	−0.38	−31.2
7. Space averaging (with boxes)	17.2	−0.44	−33.3

The point made above is important in the understanding of a Lagrangian estimate of the momentum flux across a latitude circle. For a southward flux of momentum it is required that the two horizontal components of velocity be negatively correlated. This is optimized by the components having phase relationships that places maximum and positive u and maximum and negative v in the same location in the wave. However, if these fields were sensed in a Lagrangian manner, an estimate smaller than that obtained by the Eulerian method would be expected simply because there would be fewer observations in the regions of maximum winds where the largest contribution of cross-latitude flux takes place. This most probably explains the very small momentum flux values found by Solot and Angell (1973) using GHOST data.

The method we will use to accomplish the Lagrangian-Eulerian transformation calls for a treatment of the data in such a way as to minimize its Lagrangian character and content before statistics are formed. To achieve this we will apply a straightforward averaging scheme that requires the atmosphere to be divided into longitude boxes of a suitable dimension. Later we will see that time must be added to the dimensions of the box. Suppose balloons are interrogated regularly and at each time the measurement is ascribed to the particular box into which it falls. At the end of some prescribed period a mean quantity is calculated. However, some boxes may possess more observations than others and to eliminate this bias equal weight is given to each box irrespective of the number of observations.

An understanding of the averaging scheme may be achieved by comparing Eulerian space-time means and the space and time Lagrangian means with those calculated with the box method for the simple case of a balloon at 45° whose Lagrangian motion (subscript L) is defined by

$$\left.\begin{aligned} u_L &= 16\cdot 39 + 10\sin(2\pi t/5) \\ v_L &= -5\sin(2\pi t/5) \end{aligned}\right\}, \qquad (1)$$

describing an earth orbit of 20 days with oscillations of 5 days and amplitudes of 10 and 5 m sec^{-1}, respectively.

Before proceeding, it is interesting to consider the longitudinal displacement (x) of a parcel moving in an atmosphere defined by (1) as shown in Fig. 4. Here the Lagrangian-Eulerian transformation is most apparent

as the balloon is seen to pass through successive fast and slow regions, where the residence time is in the ratio of about 1:3.

The Lagrangian time means may be defined as

$$\left.\begin{aligned}\bar{u}_L&=\frac{1}{T}\int_0^T u_L dt\\ \bar{v}_L&=\frac{1}{T}\int_0^T v_L dt\end{aligned}\right\}, \tag{2}$$

and the Lagrangian space means as

$$\left.\begin{aligned}[u_L]&=\frac{1}{X}\int_0^X u_L dx=\frac{1}{X}\int_0^T u_L^2 dt\\ [v_L]&=\frac{1}{X}\int_0^X v_L dx=\frac{1}{X}\int_0^T u_L v_L dt\end{aligned}\right\}. \tag{3}$$

It is apparent that the Lagrangian space and time means are quite different.

Besides evaluating averages using (2) and (3) for the atmospheric state defined by (1), we may also calculate means using the "box" method. To do this the 45° latitude circle is broken into 20° sections and the position and velocity of the balloon calculated every 6 hr. This provides 80 pieces of data during the 20-day orbit which are distributed unevenly in space because of the variability of the speed of the balloon. After sorting the observation to the appropriate box, calculating a mean for that box over a specific period, a zonal mean could be calculated as the average of the resultant 18 numbers.

Table 2 lists the various averages mentioned above for the atmospheric state defined by (1). The first three averages are defined by the exact integrals (2) and (3) and show a large variation between the Lagrangian space and time averages with the former appearing as the larger in both the analytic case and the numeric case where data were provided at regular intervals to simulate satellite interrogation of the balloon position. This difference is especially evident in the calculation of the Lagrangian momentum flux where $[uv]_L$ is a factor of 2 greater than the time mean $\overline{uv}_L$. Using the box-averaging scheme for Lagrangian measurements made every 6 hr, we see that there is a tendency for the time mean to be increased while the space mean is decreased. That is, the box averages lie between the extreme analytic means.

Further insight may be gained by considering the extreme states of the atmosphere of complete time dependence and complete space dependence. For the "transient" case, Dyer showed that if

$$u_E=U+u_E'(t), \quad \text{then } \bar{u}_L=U \text{ and } [u_L]>U,$$

where U is the Eulerian space-time mean, and $u_E'(t)$ the Eulerian temporal deviation from U. However for the "stationary" case, if

$$u_E=U+u_E^*(x), \quad \text{then } [u_L]=U \text{ and } \bar{u}_L<U,$$

where $u_E^*(x)$ is the spatial deviation from U.

However the real atmosphere is a complicated combination of standing and transient effects. Therefore, in order to infer the Eulerian character from the Lagrangian data, we require something midway between the two estimates, as equating the Eulerian mean to the Lagrangian time mean will, in one case, underestimate the real Eulerian mean of the mixed atmosphere. Or, on the other hand, by equating U with $[u_L]$ we would be overestimating U. Now the significance of the "box averaging" of the Lagrangian data becomes apparent as by doing this we are simultaneously carrying out a Lagrangian space and time integration. This may have been inferred from Table 2 where the production of values between the extremes of the Lagrangian space and time means by the box averaging can be seen.

b. Logistical problems

One other data reduction problem directly pertinent to the Lagrangian-Eulerian transformation evolves from the data logistics. This results from two major causes. The first is the duration of the experiment. Most balloons were released during the first three months of the experiment such that the balloon population (and therefore the observation density) reached a maximum during November; thus, the attrition rate of the balloon population was such that by June 1972, there were insufficient observations for the compilation of meaningful averages. Consequently, care had to be taken to ensure that the data-rich spring and summer months did not dominate the annual statistics.

The second logistic problem is not a function of the experiment itself but one which appears to be a property of Lagrangian tracers themselves. Table 3 shows the number of velocity observations per 10° latitude by 30° longitude box for November 1971 along 45S, and shows large variations on a day-to-day basis. Quite possibly one cluster of balloons resident in one box for one day may dominate the whole months average (e.g., day 12 in the 12th box). Up to this stage we have only considered the possibility of giving each box equal weight but have not discussed the time dimension (i.e., average period) which must be chosen to minimize the population bias described above.

The seriousness of the problem can be seen by computing zonal averages for a season using the three different time dimensions for each box i.e., one day, one month, and the whole season. The results may be seen in Table 4. Large differences are apparent in both velocity components but especially in the meridional component where there is an order of magnitude change from 0.4 m sec^{-1} (daily time dimension) to 4 m sec^{-1} (seasonal time dimension). Apparently with the longer

TABLE 3. Number of velocity determinations per 10° latitude by 30° longitude square for the month of November 1971 for 34S.

Day	Longitude box, number of 1	2	3	4	5	6	7	8	9	10	11	12	Total
1	0	9	3	15	13	31	5	10	3	8	4	0	101
2	4	3	21	3	4	2	3	1	7	12	6	5	71
3	0	8	23	14	5	11	3	0	2	4	9	2	81
4	3	3	6	4	8	13	25	18	10	1	3	2	99
5	0	0	5	24	12	5	16	29	30	6	0	5	127
6	0	1	2	5	26	16	12	20	7	8	5	0	103
7	0	0	3	1	0	4	3	7	12	16	16	1	67
8	0	0	3	0	2	13	9	13	3	6	3	5	52
9	5	5	7	2	1	2	0	1	3	0	2	0	36
10	8	8	6	8	10	23	12	7	2	2	1	8	88
11	6	4	10	0	1	2	0	2	7	2	11	1	68
12	3	16	6	7	3	2	3	3	8	2	0	23	58
13	17	11	10	4	0	1	8	4	14	19	12	5	107
14	8	4	17	26	11	17	5	28	15	15	8	7	162
15	2	2	7	20	43	12	2	8	11	4	0	8	113
16	11	7	6	21	17	11	19	8	5	10	17	2	152
17	12	15	8	25	12	25	22	5	3	3	8	20	146
18	12	6	8	7	1	0	7	6	3	1	5	8	57
19	8	19	13	29	16	7	18	13	2	0	4	1	132
20	5	17	36	25	8	7	9	5	0	0	1	2	114
21	1	7	13	23	22	35	26	4	3	4	1	1	142
22	0	7	15	7	13	37	25	6	2	7	3	3	141
23	0	3	0	8	23	26	24	17	4	8	5	1	118
24	2	6	19	5	8	16	26	15	17	12	9	3	144
25	18	10	10	4	0	1	10	26	20	25	13	9	141
26	5	2	1	4	4	8	11	17	20	7	6	4	87
27	2	0	2	2	7	8	8	10	9	10	15	2	78
28	5	2	11	22	17	24	13	13	6	8	13	15	150
29	20	5	10	28	29	15	17	15	17	13	3	13	184
30	14	2	9	12	9	19	10	27	7	11	9	12	141

time partitions, days with many observations are dominating the averages. To ease this problem, daily averages were found in each box and given equal weight in the compilation of longer term means. Boxes containing no balloons on a particular day were assigned an interpolated value based on an upstream and downstream value.

In summary, the averaging scheme used gives equal weight to daily averaged quantities in each longitude-latitude box, providing a grid of approximate Eulerian values for each day of the EOLE period. The box scale chosen for this study was 30° longitude and 10° of latitude.

4. Time sections

The variation of the zonal average of an atmospheric variable, averaged in time over the period of a day, may be a complicated function of both latitude and time. Such a distribution is illustrated in Fig. 5, which shows the time section of the zonally averaged eastward velocity component near 200 mb from 11 November 1971 through 11 January 1972. Zones of relatively strong westerlies are seen to vary from latitude to latitude with periodicities of from days to weeks. Webster and Keller (1974) show definite rhythms existing in the zonal flow and the energetics, principally on the time scale of 18–23 days. However, we will deal here with variations over a time scale significantly larger with a lower limit of the order of a month. In order to concentrate on variations of this longer time scale, means of the order of a month are used in all quantities studied in this section.

TABLE 4. Comparison of $[\bar{u}]$ and $[\bar{v}]$ at 45S using equally weighted 30° boxes in longitude but three different time partitions.

Averaging method	$[\bar{u}]$ (m sec^{-1})	$[\bar{v}]$ (m sec^{-1})
Equal daily weight	30.7	0.4
Equal monthly weight	29.6	2.5
Seasonal average (no weight)	29.0	4.0

The notation used is described briefly below. If there are two quantities X and Y which are resolvable into space and time means plus the deviations from those means, i.e.,

$$\left.\begin{aligned} X(x,y,t)&=\bar{X}(x,y)+X'(x,y,t)\\ X(x,y,t)&=[X(y,t)]+X^*(x,y,t), \text{ etc.}\end{aligned}\right\}, \tag{4}$$

where ($\bar{\ }$) denotes a time-mean and ($'$) the time deviation, and ([ ]) the zonal or longitudinal average and (*) the space deviation, it is simple to show that

$$[\overline{XY}]=[\bar{X}][\bar{Y}]+[\overline{X^*Y^*}]+[\overline{X'Y'}]. \tag{5}$$

The total flux $[\overline{XY}]$ is made up of contributions from the zonally averaged flow, the standing or geographically fixed eddies, and the transient eddies, respectively.

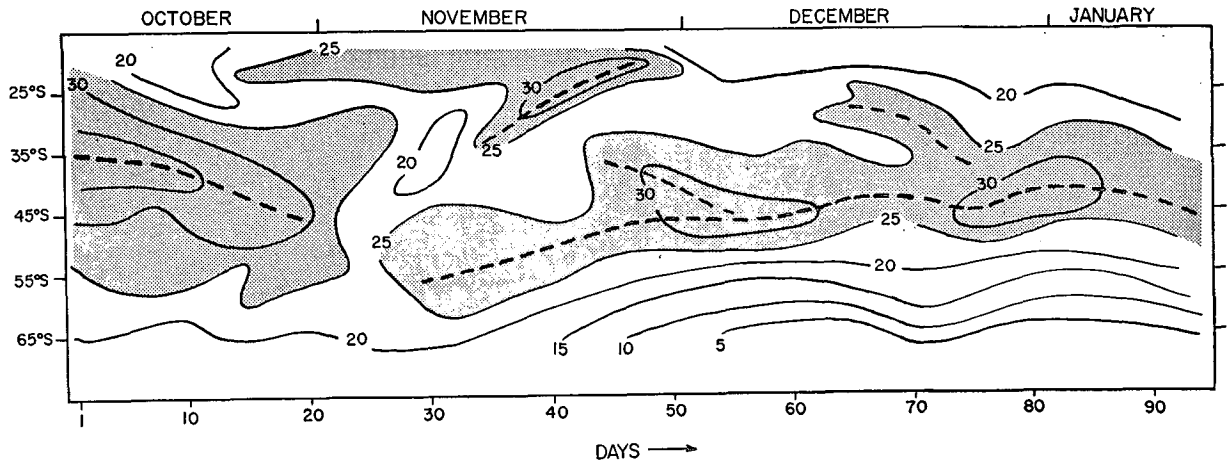

FIG. 5. Three-day running mean of the zonally averaged eastward velocity component of velocity (m sec^{-1}). Dashed lines represent the axes of the various maxima.

The time section for $[\bar{u}]$, using the time unit of one month, is shown in Fig. 6 for the entire EOLE period as a function varying smoothly in time and latitude. The spring months SON (Sept., Oct., Nov.) are characterized by a broad and strong band of westerlies with maximum winds in the subtropics with magnitudes of about 35 m sec^{-1}. During the summer months the band of westerlies has contracted and moved poleward with weaker adjacent zonal winds. Through autumn (MAM) and toward winter (JJ), the westerlies again intensify and move considerably equatorward.

van Loon *et al.* (1972) show the latitudinal distribution of the $[\bar{u}]$ field estimated geostrophically from the available Eulerian data for both the Southern Hemisphere summer and winter. The position of the summer maximum agrees quite well with the EOLE estimate with a similar magnitude of about 30 m sec^{-1}, decreasing swiftly equatorward and poleward. Likewise, there is excellent agreement with the positioning of the winter maximum which is considerably equatorward of the summer position, as we have seen in Fig. 6. Importantly, both estimates show a general broadening of the westerly maximum. The similarity for the two time periods adds credence to the variation of $[\bar{u}]$ over the entire year, as suggested by the EOLE data analysis.

Even with the dense EOLE data there is difficulty in resolving the zonal mean of the meridional velocity component $[\bar{v}]$. This is, of course, a consequence of the smallness of the quantity resulting from the averaging of very large numbers of different signs all of which contain observational error. The major effect of the closeness to zero of $[\bar{v}]$ is to reduce the region of interpretation to between about 25–65S where the data density is maximum. Outside these regions there exists sufficient longitudinal bias in the data to suggest an uncertainty in the exclusion of $[\bar{v}]$ from zero. The resultant distribution of $[\bar{v}]$ is shown in Fig. 7 with the dashed lines showing estimates rendered questionable by insufficient data.

The distribution of $[\bar{v}]$ appears to fit with the distribution of the various traditional branches of the meridional circulations. In the latitude belt 25–65S we see that in the spring $[\bar{v}]$ is generally positive (northward) in mid-latitudes and negative (southward) farther poleward. These may be labelled, respectively, the upper tropospheric branches of the Ferrel circulation and the polar circulation. Through the summer the Ferrel cell appears to move poleward to be replaced in the subtropics by a band of southward (negative) winds representing the southward extension of the Hadley circulation. Autumn finds a return to the spring situation, although with smaller amplitude. The estimates of Obasi (1963) and Gilman (1965) agree in form to those presented here although a factor of 2 smaller. Irrespective of this agreement, the variation of $[\bar{v}]$ remains a most uncertain field.

The time section of temperature is shown in Fig. 8. In the subtropics the variation through the year is generally small, with anomalies of only 4C. However, more poleward, there exists an annual variation of a

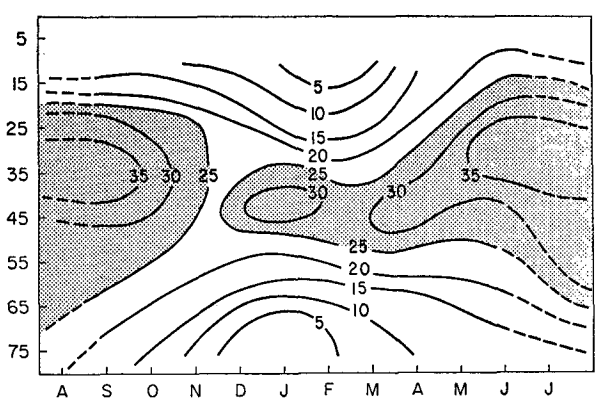

FIG. 6. Time section of the mean monthly zonally averaged eastward velocity component plotted as a function of latitude. Shaded regions denote magnitudes of 25 m sec^{-1} and dashed lines suggest regions of sparse data.

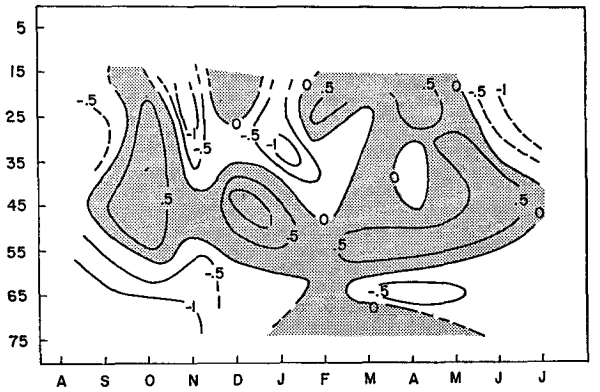

FIG. 7. As in Fig. 6 except for the mean meridional velocity component. Shaded regions denote a northward (positive) component.

much greater magnitude with winter and spring temperatures near 70S of −65 to −70C, warming rapidly through the spring to −40C with a maximum rate of warming occurring in November. This corresponds to the spring stratospheric warming of the polar regions in the Southern Hemisphere which is substantially weaker than its Northern Hemisphere counterpart (van Loon *et al.*, 1972). The warming continues at a slower rate through the summer to result in a reversal of the latitudinal temperature gradient.

The major differences between the most recent conventional estimates of the mean temperature field (van Loon *et al.*) and that shown in Fig. 8 appear in the magnitudes of the cold winter temperatures in the Antarctic region. This region corresponds to one of the more adequately observed areas of the Southern Hemisphere by conventional techniques but relatively sparsely by the EOLE system (see Fig. 2). Because of this, and the averaging scheme used, the EOLE estimates will be influenced by balloon observations of temperatures to the north, biasing the observations toward higher and warmer averages than would be reported by individual Antarctic observing stations.

The annual variation of the northward momentum and sensible heat fluxes, due to transient eddies as defined in (7), is shown in Figs. 9 and 10. We have not included the variation of the momentum flux contributions of the mean flow or standing eddies, because of their relative smallness in the Southern Hemisphere. This point will be discussed further in the next section.

Two major momentum flux regimes may be seen to exist throughout the entire year with a line of demarkation between 50–55S. This boundary separates the strong southerly flux (negative) and the northward flux (positive and shaded), the former being the much stronger of the two. Whereas there appears to be relatively little change in magnitude of the negative maximum, there is a general position trend through the year similar to that noted in the $[\bar{u}]$ section of Fig. 6. A closer comparison of the two reveals that the maximum southward flux of momentum occurs generally to the equatorward of the $[\bar{u}]$ maximum. This corresponds to a convergence of momentum into the mean westerlies from the north and by the transient eddies. Similarily, the smaller northward flux lies to the south of the jet stream, again suggesting a convergence of momentum into the jet from the south. Although we will discuss the conversion of energy from one form to another in the next section, it would appear that the transient eddies may be maintaining the zonal mean westerlies thus substantiating many studies using conventional data.

As with the momentum flux, two major regimes appear in the distribution of the sensible heat flux by the transient eddies. Generally in the south there is a weak but substantial region of positive heat flux with a stronger band of negative flux more equatorward. The exception to this occurs in the late winter and early spring which possesses an intense negative flux in the middle and high latitudes. Considering the period from late August through November, we find that the strong negative heat flux corresponds in location (latitude and time) to the extreme cold Antarctic winter air (Fig. 8). Presumably the eddies are transporting anomalously warm air from lower latitudes ($T'>0$) southward ($v'<0$), resulting in $[\overline{v'T'}]<0$. In this manner, the flux of heat down the temperature gradient is an attempt by the eddies to reduce the mean temperature gradient and, therefore, the available potential energy of the mean zonal flow. Thus, in this region and period of the year, the transient eddies are working to break down the mean zonal temperature gradient in a manner that differs dramatically from that suggested by their momentum flux properties.

However, the role of the transient eddies changes following the late spring warming of the upper troposphere and lower stratosphere. With the accompanying reversal of the mean temperature gradient, the continuing negative flux suggests the possibility of a refrigeration process, with the already warm high latitudes being further heated by the advection of en-

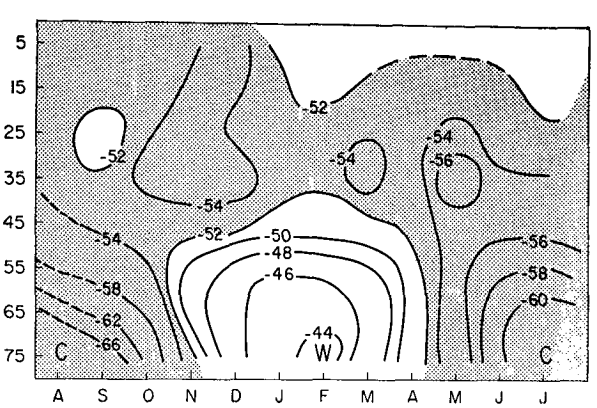

FIG. 8. As in Fig. 6 except for the zonally averaged temperature (°C). Shaded area denotes region cooler than −52C.

thalpy by the transient eddies. In this season the transient eddies act to increase both the available potential energy and the kinetic energy of the mean zonal flow.

5. Hemispheric energetics

a. The momentum budget

A momentum budget for the entire EOLE period and for each season is shown in Fig. 11. The budget for JJA is doubtful for all latitudes and is included here only to complete the annual sequence.

In the upper portion of each diagram are the zonal averages of the total northerly momentum flux $[\overline{uv}]$, the eastward velocity component $[\bar{u}]$ and their angular counterparts $[\overline{uv}]_A$ and $[\bar{u}]_A$. In order to use the same scale as the linear quantities, a proportionality factor of the radius of the earth (a) has been omitted so that the relationships are given by

$$\left.\begin{aligned}[\bar{u}]_A&=[\bar{u}]/\cos\phi\\ [\overline{uv}]_A&=[\overline{uv}]\cos^2\phi\end{aligned}\right\}, \tag{6}$$

where ϕ is the latitude. Consequently, the magnitude of the "angular" velocity will exceed $[\bar{u}]$ at all latitudes whereas the "angular" momentum will be less than its linear counterpart. This has the effect of shifting the linear momentum maximum equatorward and the velocity maximum poleward to such latitudes that there exists, in the mean, a convergence of momentum into the mean westerly maximum. This occurs in all seasons with the large southward (negative) momentum flux in the subtropics and mid-latitudes and the weaker northward flux (positive) from high latitudes being the major contributors to the momentum convergence.

Such a momentum distribution has an important dynamic consequence and represents the conversion of perturbation or eddy kinetic energy (K_E) to kinetic energy of the mean zonal flow (K_Z). This well-known

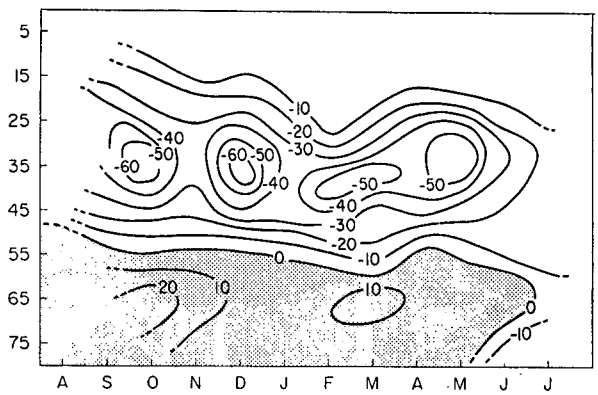

FIG. 9. As in Fig. 6 except for the northward momentum flux (m^2 sec^{-2}) due to transient eddies. Shaded regions denote northward flux.

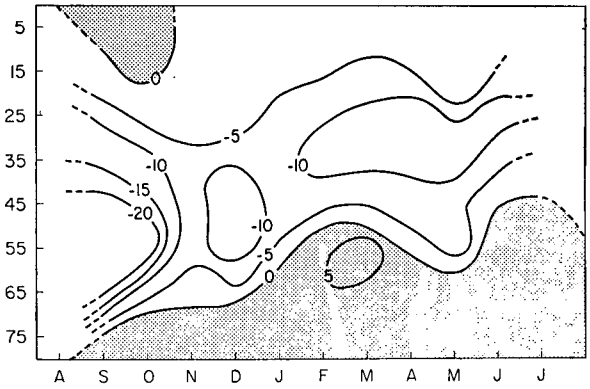

FIG. 10. As in Fig. 6 except for the northward flux of sensible heat (°K m sec^{-1}) due to transient eddies.

energy conversion term may be written as

$$\{K_E\cdot K_Z\}\alpha-([\overline{u'v'}]+[\overline{u^*v^*}])\cos^2\phi\frac{\partial}{\partial\phi}\frac{[\bar{u}]}{\cos\phi}, \tag{7}$$

which is positive for maintenance of the mean flow at the expense of the eddies but negative for the reverse process. For consistency with the "angular" velocity and momentum terms shown in Fig. 11, a factor of a^{-2} has been omitted in (7). On a day-to-day basis this term varies rapidly in sign although in higher latitudes it has been shown to possess a strong 18–23 day periodicity (Webster and Keller, 1974). However, in the mean, it is apparent that this term is positive as can be seen by the mean components of (7) in Fig. 11. That is, generally $[\overline{uv}]$ is negative when $[\bar{u}]$ decreases toward the equator while $[\overline{uv}]$ is positive when $[\bar{u}]$ increases with decreasing latitude.

A time section of the barotropic energy conversion may be seen in Fig. 12 for the entire EOLE period. The most important feature is the meandering positive maximum which follows the progression of the westerlies although just equatorward (Fig. 6). Immediately poleward is a weak negative band denoting a mean trend in the reverse direction. Farther south, the sense changes once again and the conversion is positive, reflecting the weak northerly momentum flux from higher latitudes.

In Fig. 6 we noted that the intensity of the mean zonal flow is weaker in summer and it appears inconsistent that there is a strong positive maximum of $\{K_E\cdot K_Z\}$ during this season. However, this results from the gradient of $[\bar{u}]$ increasing as the mean jet becomes narrower and weaker. This, plus the only slightly smaller value of the transient momentum flux (Fig. 9), which also has moved farther south, provides a large positive conversion of kinetic energy from the eddy to the mean zonal form.

Returning to Fig. 11, we can identify the major atmospheric mode types that contribute to the total

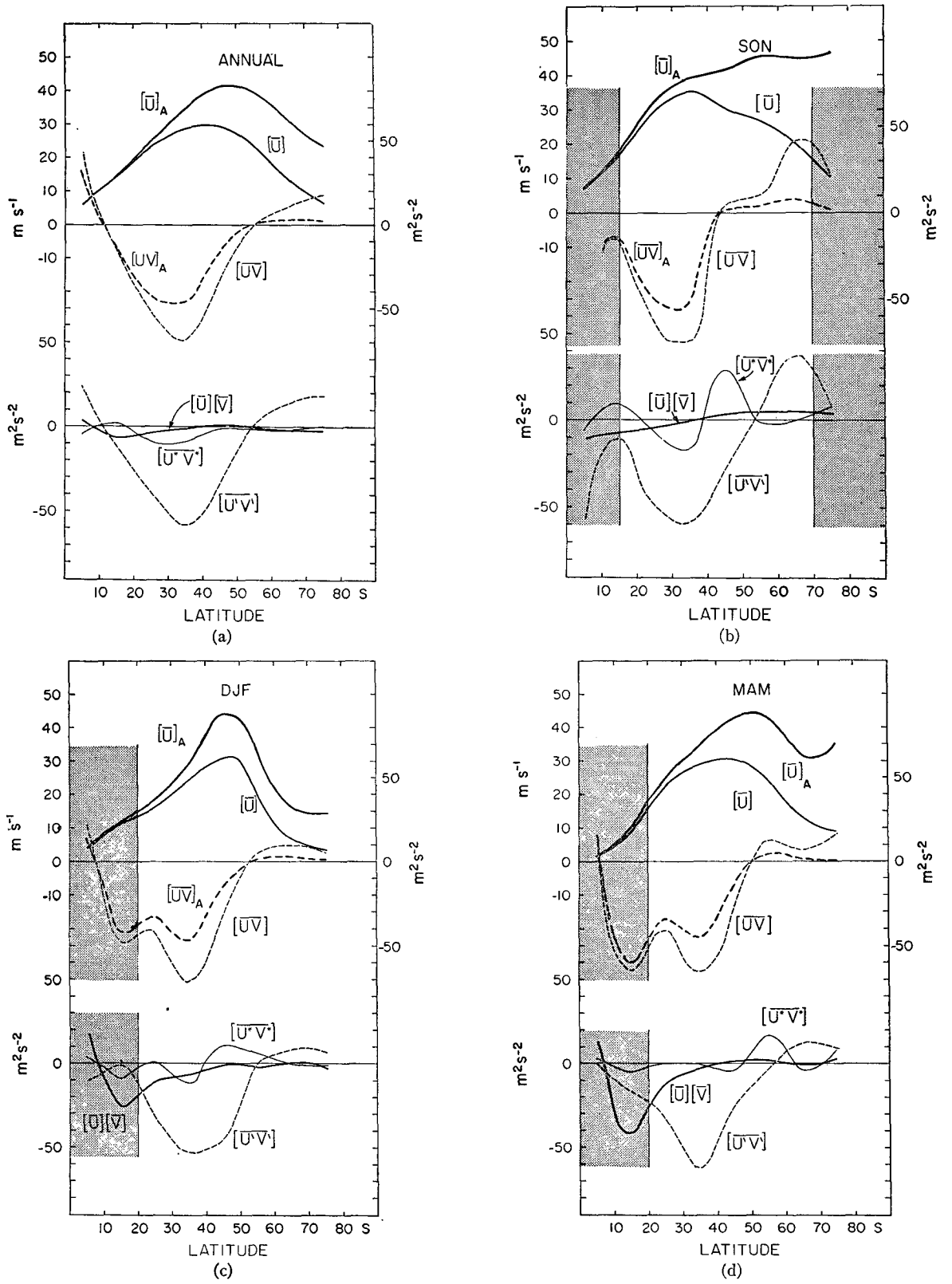

FIG. 11. Latitudinal distribution of the components of the total northward momentum flux $[\overline{uv}]$ with the notation given in Eq. (5) for (a) the total EOLE period (annual), (b) Sep.–Nov., (c) Dec.–Feb., (d) Mar.–May and (e) Jun.–Aug. Components are plotted in the lower diagram. Upper diagram shows the total momentum (subscript A denotes "angular" quantity) on the right-hand scale, and the mean zonal velocity $[\bar{u}]$ on the left. Regions outside the vertical bar denote regions of sparse data.

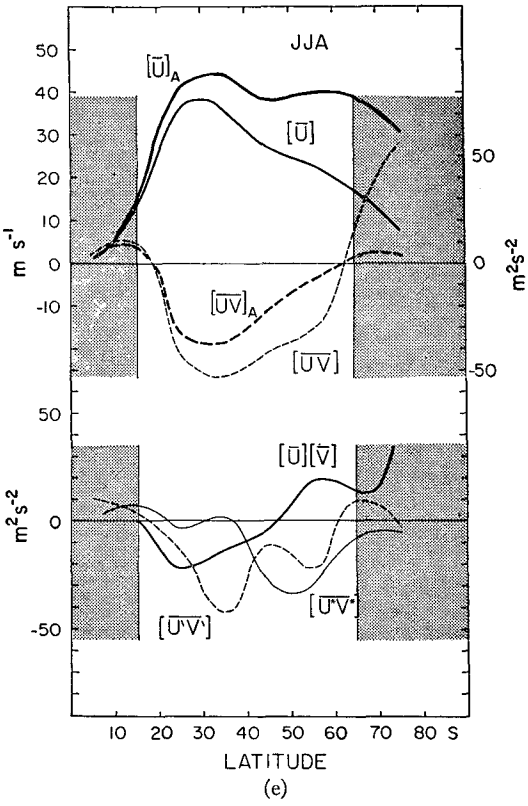

FIG. 11. *Continued*

momentum flux, and, consequently, to the conversion of one form of kinetic energy to the other. This breakdown is shown in the lower portion of Fig. 11 where the magnitudes of the three momentum forms defined in (5) are plotted against latitude. Ignoring the regions of relatively poor data (shaded regions) and JJA, we we find that in all seasons that the transient eddies tend to dominate, except perhaps in SON where the effect of the standing eddies seems to be somewhat more important than in the other seasons. Whereas the local transport of the standing eddies may be large and nearly equal to that of the transient waves, most of this cancels out in the zonal mean so that the total transport across a latitude circle is generally small. The spatial nature of all quantities will be concentrated on in Webster and Curtin (1974).

A comparison of the sensible heat flux due to the standing and transient eddies is shown in Fig. 13. Here again, in all regions and periods of dense data, the transient eddies provide the majority of the sensible heat flux. Generally there exists a large negative maximum centered near 45–50S, decreasing rapidly both equatorward and poleward. This may be explained as the transport of anomalously warm air southward or anomalously cold air northward. Whether this means that the eddies are transporting heat to warm or cold regions depends upon the distribution of the zonally averaged temperature which is shown in the upper part of each diagram. For example, the temperature profile in DJF increases through the mid-latitudes toward the poles, providing a strong negative temperature gradient. In this region the eddies possess a strong negative flux signifying that they are transporting the anomalously cold air of the subtropics in order to decrease the mean temperature gradient. This would have effect of decreasing the mean potential energy of the hemisphere, suggesting that the eddies are, in this season, depleting the energy of the mean flow while at the same time increasing their own potential energy.

The conversion between the available potential energies of the mean zonal flow (A_Z) and the eddies (A_E) may be written as

$$\{A_Z \cdot A_E\}\alpha -([\overline{v'T'}]+[\overline{v^*T^*}])\frac{\partial}{\partial\phi}[\bar{T}], \qquad (8)$$

which is positive when the eddies transport enthalpy down the mean temperature gradient thus minimizing the zonal available potential energy. On the other hand, the potential energy of the eddies is reduced in favor of A_Z when the eddies tend to transfer sensible heat against the gradient, warming already warm regions or cooling already anomalously cool regions.

The variation of the $\{A_Z \cdot A_E\}$ energy conversion through the year may be seen in Fig. 14 where two major regimes are evident. In the spring months and in middle and high latitudes there is an intense region of positive conversion where evidently the eddies are gaining potential energy at the expense of the mean flow. This is being accomplished by a flux of sensible heat by the eddies from the warmer mid-latitudes into the very cold polar regions.

From Fig. 13 we can see that whereas the flux of sensible heat by the transient eddies remains strong and southward into the Southern Hemisphere summer the northward temperature gradient changes sign following the spring warming. These two factors together produce the large and negative $\{A_Z \cdot A_E\}$ in the mid-latitudes of early summer. The strong refrigeration process decreases through summer and into autumn.

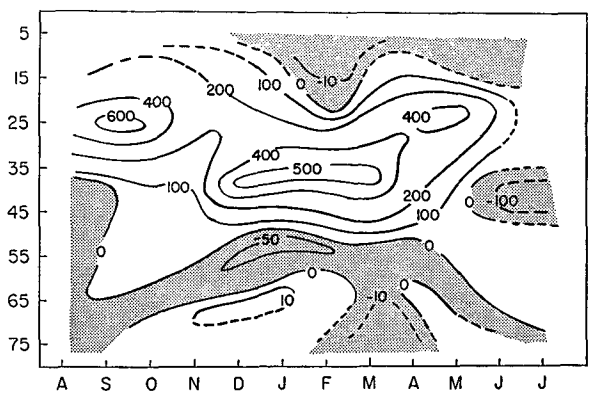

FIG. 12. Time section of the mean kinetic energy conversion $\{K_E \cdot K_Z\}$ as a function of latitude. Shaded areas denote a negative conversion (units: m^3 sec^{-3}).

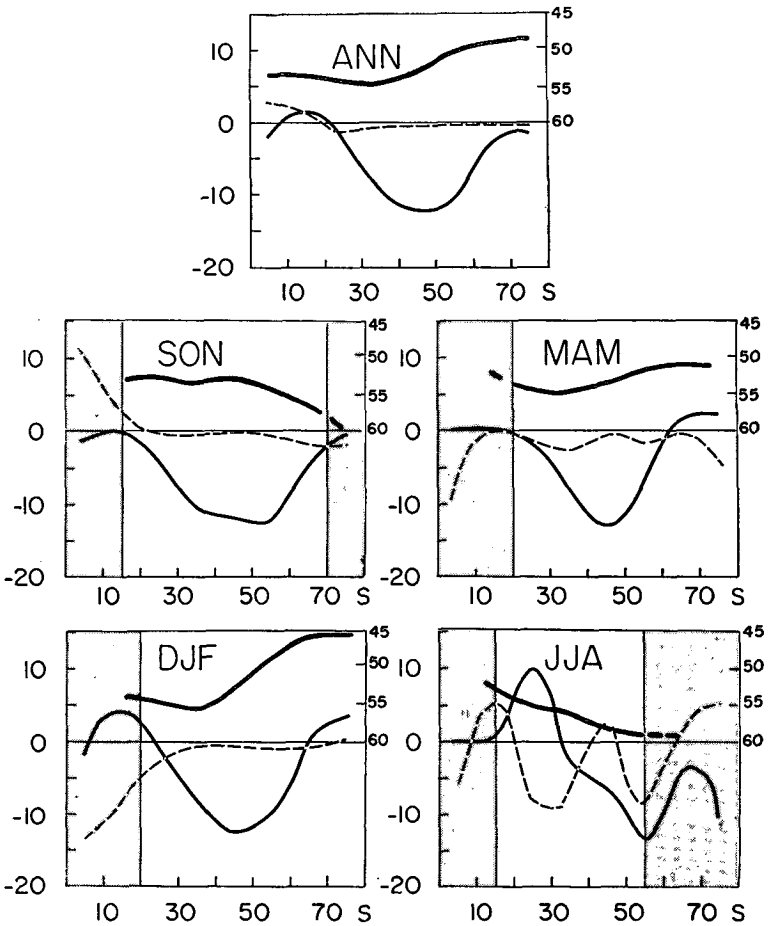

FIG. 13. Comparison of the sensible heat flux due to transient eddies (solid curves) and standing eddies (dashed) as a function of latitude and season. Heavy solid line denotes the mean zonal temperature relative to the right-hand scale (units: °K m sec^{-2} and °C, respectively).

At lower latitudes and throughout the EOLE period there exists a weak positive band of energy conversion.

6. Comparisons and conclusions

With information from only one level in the atmosphere and that coming from the upper troposphere, it is difficult to draw too many conclusions regarding the total energy balances or fields of motion of a hemisphere. However, the analyses presented in the preceding sections do contain major differences in form and magnitude when compared with those resulting from conventional Eulerian data sets and also the earlier Lagrangian estimates. These differences are of sufficient magnitude as to warrant discussion and resolution in order to determine whether they are data-source dependent or real.

One of the most interesting features of the EOLE analyses is the absence of any double maximum in either the annual variation of $[\bar{u}]$ (Fig. 6) or in its seasonal means (Fig. 11). This omission in the data has important consequences in the understanding of the structure of the so-called Sub-Tropical Jet Stream (STJ) of the Southern Hemisphere. Early studies (e.g., Obasi, 1963) contend that the STJ exists as an entity girdling the subtropics equatorward and separate from the middle-to-high-latitude zonal wind maximum. This contention was recently discussed by Newton (van Loon *et al.*, 1972) and the question of there being only one or a multiple of mean jet maxima was considered to be still unresolved.

Table 5 presents a seasonal comparison of the latitudinal structure of $[\bar{u}]$ derived from various sources. As may be seen in Fig. 11, the EOLE results suggest a broad westerly maximum throughout the year that meanders generally equatorward in winter and poleward in summer. Such a structure is reflected in the averages of Newell *et al.* (1972). However in JAA Obasi (1963) suggests a decidedly double maximum in $[\bar{u}]$. Also contrary to the EOLE results are those compiled by Solot and Angell (1969b) which also show a double maximum, but with the northerly maximum removed substantially equatorward to that of Obasi.

Considering first the results of Solot and Angell (1969b), it is interesting to note that equatorward of 35S their averages bear little resemblance to any of the other three estimates during any season. An investigation of the distribution of the GHOST data (Table 2 of Solot and Angell, 1969a) shows the regions of anomalous values correspond to regions of minimum data. In fact, the zonal averages at 20 and 25S were based on 12, 7, 40 and 14 and 4, 2, 18 and 11 sets of 24-hr average velocities, respectively, during the seasons DJF, MAM, JJA and SON. However, the mere lack of data is not in itself an explanation of the large values of zonal wind in this region. To explain this we must ask the question of why there are so few observations in this locality. This may be explained in the following manner. The population of GHOST balloons indicated a general migration poleward during spring and summer followed by an equatorward movement in autumn and winter. This mass drift of the population moves the latitude of maximum observations in the same fashion, resulting, in spring and summer, in very few observations and therefore very few velocity determinations in the subtropics and low latitudes. Consequently, only balloons that are rapidly advected out of the mid-latitudes (by large-scale disturbances) may be sensed in the subtropics during this time. Similar occurrences are apparent in the EOLE experiment where, associated with such disturbances, are extremely strong westerlies. Thus, rather than sensing the mean wind, balloons at low latitudes tend to sample the intense westerlies of individual disturbances during their rapid excursion toward the equator before being returned to higher latitudes.

For the above reason it is likely that the low-latitude estimates of $[\bar{u}]$ from the EOLE data set are similarly overestimated, although with a larger population of balloons more eddies would tend to be sampled which may have reduced the average value. Also with more balloons entering the low latitudes, the probability of balloons disassociating themselves from the disturbances increases and in this manner may have provided a more representative value of the mean condition.

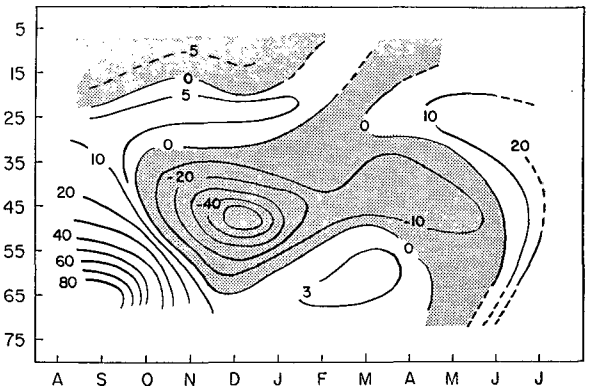

FIG. 14. Time section of the mean available potential energy conversion $\{A_Z \cdot A_E\}$ as a function of latitude. Shaded areas denote a negative conversion [units: m (°K)^2 sec^{-1}].

Even so, the value of a balloon system with release stations in middle and high latitudes, as a source of representative data for low latitudes, is highly questionable. Even with release stations located in the tropical latitudes (as is proposed in the TWERLE experiment), the balloons may only be expected to be representative of the mean tropical atmosphere while they remain within the tropics and before the migration of the population toward mid-latitudes.

An explanation of why Obasi (1963) may have sensed a double maximum must await the second part of this study (Webster and Curtin, 1974) where the longitudinal structure of $\bar{u}$ is discussed. There it will be shown that the STJ is an intense part of the basic westerly maximum, which during the Southern Hemisphere winter (JJA) extends northward over the Australian sector while remaining well poleward at all other longitudes. With summer comes a weakening and a retreat poleward with the maximum extending over a wide longitudinal arc through the South Pacific and Atlantic Oceans. Quite probably Obasi's double winter maximum may be merely a manifestation of the Eulerian spatial bias arising from clusters of stations, geographically biased, being used to compute a zonal mean.

TABLE 5. Estimates of $[\bar{u}]$ compiled by Obasi (1963), Solot and Angell (1969b) and Newell *et al.* (1972) compared with estimates obtained from the EOLE data set for Dec.–Feb., Mar.–May, Jun.–Aug. and Sep.–Nov. Values in parentheses refer to values at 20S instead of 15S.

	a. DJF Latitude (°S)						b. MAM Latitude (°S)					
	15	25	35	45	55	65	15	25	35	45	55	65
EOLE	10.3	15.0	24.9	30.4	19.2	6.2	8.9	21.0	29.2	30.3	25.0	13.5
Obasi	9.2	19.7	24.7	24.7	23.5	14.4	—	—	—	—	—	—
Newell *et al.*	3.5	14.2	21.8	22.0	17.2	10.0	10.4	20.7	23.3	21.2	18.1	13.1
Solot-Angell	(26.7)	27.3	20.3	25.6	21.3	10.0	(26.7)	29.0	29.0	27.7	22.7	18.0
	c. JJA						d. SON					
EOLE	12.4	35.0	37.5	27.5	23.9	18.4	16.2	28.7	35.0	30.4	27.7	20.4
Obasi	12.0	31.1	30.8	22.0	29.7	19.4	—	—	—	—	—	—
Newell *et al.*	12.7	26.5	27.9	23.2	21.2	16.4	11.6	22.7	24.0	22.0	19.5	13.9
Solot-Angell	(44.0)	40.0	34.3	29.7	21.7	17.7	(39.0)	32.3	27.0	30.3	25.3	18.7

TABLE 6. Estimates of $[\overline{u'v'}]$ compiled by Obasi (1963), Solot and Angell [(i) 1969b and (ii) 1973] and Newell *et al.* (1972) compared to those obtained from the EOLE set for Dec.–Feb., Mar.–May, Jun.–Aug. and Sep.–Nov. Solot and Angell's (ii) estimates refers to a mid-latitude average value.

	a. DJF Latitude (°S)						b. MAM Latitude (°S)					
	15	25	35	45	55	65	15	25	35	45	55	65
EOLE	− 3.2	−28.0	−50.0	−47.5	− 3.4	10.0	−18.0	−32.9	−61.2	−25.0	− 4.0	11.5
Obasi	− 6.2	−28.1	−46.6	−41.9	−22.3	0	—	—	—	—	—	—
Newell *et al.*	−14.0	−32.4	−45.6	−31.8	− 7.8	6.5	−16.9	−37.1	−46.1	−32.7	−11.3	7.0
Solot- (i)	—	—	−12.7	− 6.0	3	4.3	—	—	−15.3	−10.0	− 1.0	.7
Angell (ii)				(−3)						(−4)		
	c. JJA						d. SON					
EOLE	2.1	−11.5	−42.3	−13.0	−22.0	9.8	−10.8	−47.5	−59.9	−29.9	5.0	36.5
Obasi	− 1.3	−25.3	−34.4	−22.8	− 3.8	14.1	—	—	—	—	—	—
Newell *et al.*	− 5.2	−31.3	−39.6	−21.7	− 0.2	16.0	−10.0	−31.1	−43.4	−34.4	−11.4	10.4
Solot- (i)	—	−24.0	−14.7	− 8.3	− 2.7	− .7	—	—	−11.7	− 5.3	0	− 2.0
Angell (ii)				(−6)						(−5)		

This may be seen by comparing the distribution of Southern Hemisphere stations (Table 1) and Obasi's estimates of $[\bar{u}]$ (Table 5) in conjunction with the longitudinal description of $\bar{u}$ given above. From this we can see that in JJA the observing system would sense the intense maximum over Australia. Similarly, stations in South America and South Africa would sense the poleward parts of the meandering stream. Between these extreme latitudes the jet tends southward but as this takes place principally over the ocean the sensed distribution would possess two maxima. This explanation is supported by the absence of a double jet in Obasi's DJF estimate which is replaced by a very broad and weaker profile. This appears consistent with the sensing of the weaker and more southerly position of the jet over Australia given the clustering of the conventional data stations.

The results of this study tend to support a much simpler picture of the mean upper troposphere circulation with only one mean jet stream which meanders latitudinally and varies in magnitude as a function of the time of year. Indeed, the latitudinal variation of the momentum flux (Figs. 8 and 11) adds consistency to this simple picture and allows us to avoid the difficult question of how a mean double maximum could be supported and maintained energetically.

Besides differences in the distribution of $[\bar{u}]$, there exist large differences in the magnitudes between the EOLE estimates and those of Newell *et al.* Generally the former exceeds the latter at all latitudes with a maximum departure exceeding 10 m sec^{-1} at 35S in JJA and SON. Whereas the difference in the JJA estimates could be attributed to the poor EOLE data in this season, it must be remembered that during SON the EOLE data are most abundant at this latitude. Three possibilities that may account for these differences come immediately to mind. These are that the Newell *et al.* data period was much longer and did not include the EOLE period, that conventional data resulted in an underestimate of the zonal averages, or that the Lagrangian system overestimates the zonal averages.

The first explanation appears unlikely in that while year-to-year differences do occur in mean zonal averages (e.g., Obasi and Newell *et al.* are quite different), it is difficult to account for the maximum 10 m sec^{-1} in this way. More likely it is that one of the data sources either overestimates or underestimates the average. A Eulerian underestimate would result from either a sampling bias or by the method of interpolation used in regions of poor data. But such bias could equally result in an overestimate. This point will be discussed in Webster and Curtin (1974). However, it should again be pointed out that geostrophic estimates by van Loon *et al.* do suggest more intense values than do those of Newell *et al.*, i.e., summer maxima of 30 m sec^{-1} at 45S and 40 m sec^{-1} at 30S, values which are very similar to the EOLE estimates. However it is as difficult to understand the differences between the various Eulerian estimates as it is to assimilate the EOLE means.

The third possibility, that the EOLE system overestimates the zonal mean, is a very difficult question to resolve. Such an overestimate could arise if, for example, the balloons tended to follow, and thus over-sample, the jet streams. The averaging scheme developed in this paper was aimed at eliminating such problems by equally weighting each box. In fact, the number of balloons in each box during November (Table 2) has near zero correlation with the *resultant* daily mean wind speed.

A comparison of various estimates of the northward momentum flux due to the transient eddies is shown in Table 6. Comparing first the Eulerian and EOLE covariances, it is probable that the differences may be explained by the same reasoning employed in the discussion of the $[\bar{u}]$ fields. This is because the Eulerian covariances were calculated relative to the same distribution of observing stations. However, despite specific differences the estimates are of the same magni-

tude and show similar variation with latitude. Of course, this does not include the JJA fields where the large disparity is due to the sparse EOLE data which has become much more apparent in the calculation of a covariance.

Such similarities, however, are by no means evident in the Solot and Angell estimates (1969b, 1973) which are at least a factor of 4 smaller than either the EOLE or Eulerian values. This disparity was pointed out earlier as an example of Lagrangian temporal bias (Section 3) and illustrates the care that must be taken in estimating Eulerian quantities from Lagrangian information.

It should be mentioned that at least some of the underestimation of the momentum flux by Solot and Angell could have resulted from the fact that the GHOST velocities were obtained from 24-hr balloon displacements, producing not 2-hr average velocities as in the EOLE data set or instantaneous velocities as would result from conventional data, but 24-hr average winds. However, as much of the cross-latitude momentum flux is accomplished by waves with periods of 4–6 days, it would appear that this would not result in a major part of the underestimation.

In conclusion, it appears that balloon systems such as that used in the EOLE system are quite capable of providing large quantities of data which if defined appropriately and treated in the proper manner may be used to infer useful information relating to the mean structure of the atmosphere. Most importantly, the cloud of unrepresentativeness lowered over Lagrangian data by Solot and Angell's momentum flux interpretations from the GHOST data, may be at least partially eliminated by the results presented here, which were arrived at by a systematic application of Dyer's considerations.

Acknowledgments. The authors are indebted to W. R. Bandeen of the NASA Goodard Space Flight Center for his help and encouragement during the course of this study. Calculations were made using the IBM 360/91 of the UCLA Central Computing Network. This research was supported by NASA Grant NGR 05-007-091.

REFERENCES

Angel, J. K., 1972: Some climatological aspects of circulation in the Southern Hemisphere temperate latitudes as determined from 200 mb GHOST balloon flights. *Mon. Wea. Rev.*, **100**, 107–116.

Dyer, A. J., 1973: Do GHOST balloons measure Eulerian mean velocities? *J. Atmos. Sci.*, **30**, 510–513.

Gilman, P. A., 1965: The mean meridional circulation of the Southern Hemisphere inferred from momentum and mass balance. *Tellus*, **17**, 277–284.

Morel, P., and W. R. Bandeen, 1973: The EOLE experiment: Early results and current objectives. *Bull. Amer. Meteor. Soc.*, **54**, 298–305.

——, and G. Necco, 1973: Scale dependence of the 200-mb divergence inferred from EOLE data. *J. Atmos. Sci.*, **30**, 909–921.

Newell, R. E., J. W. Kidson, D. G. Vincent and G. J. Boer, 1972: *The General Circulation of the Tropical Atmosphere and Interactions with Extratropical Latitudes*, Vol. 1. The MIT Press, 258 pp.

Obasi, G. O. P., 1963: Atmospheric momentum and energy calculations for the Southern Hemisphere during the IGY. Planetary Circulations Project, MIT, 353 pp.

Solot, S. B., and J. K. Angell, 1969a: Temperate latitude 200-mb zonal winds from GHOST balloon flights in the Southern Hemisphere. *J. Atmos. Sci.*, **26**, 574–579.

——, and ——, 1969b: Mean meridional air flow implied by 200-mb GHOST balloon flights in temperate latitudes of the Southern Hemisphere. *J. Atmos. Sci.*, **26**, 1299–1305.

——, and ——, 1973: The mean upper-air flow in the Southern Hemisphere temperate latitudes determined from several years of GHOST balloon flights at 200 and 100 mb. *J. Atmos. Sci.*, **30**, 3–12.

van Loon, H., J. J. Taljaard, T. Sasamori, J. London, D. V. Hoyt, K. Labitzke and C. W. Newton, 1972: *Meteorology of the Southern Hemisphere, Meteor. Monogr.*, **13**, No. 35, 263 pp.

Webster, P. J., and J. L. Keller, 1974: A strong tropospheric and stratospheric rhythm in the Southern Hemisphere. *Nature*, **248**, 212–213.

——, and D. G. Curtin, 1974: Interpretations of the EOLE experiment: II. Spatial variation of Eulerian quantities (in preparation).